Growth of Ag on Cu(100) studied by STM: From surface alloying to Ag superstructures

P. T. Sprunger,* E. Lægsgaard, and F. Besenbacher
Institute of Physics and Astronomy and Center for Atomic-scale Materials Physics (CAMP), University of Aarhus DK-8000 Aarhus C, Denmark
(Received 1 May 1996)

The nucleation and growth of Ag on Cu(100) and the resulting surface structures have been studied with variable temperature (150–330 K) scanning tunneling microscopy (STM). At temperatures below 250 K, islands of Ag, having a pseudohexagonal, $c(10\times2)$ *overlayer* structure, nucleate and grow on Cu terraces and at step edges at Ag subsaturation coverages. However, at temperatures at or above 300 K, a substitutional Ag-Cu surface alloy forms, showing that the formation of the surface alloy phase is an activated process. It is found that only a limited amount of Ag (~0.13 ML) can be accommodated *within* the Cu(100) surface layer. At higher coverages ($0.13\ \text{ML} \leqslant \theta_{\text{Ag}} < 0.9\ \text{ML}$), the strain energy induced by the alloyed Ag becomes so high that the Ag atoms segregate into small patches of $c(10\times2)$ superstructure located within the Cu surface layer. Upon Ag deposition at or above the first monolayer at 425 K, a simple pseudohexagonal *overlayer* structure is observed, indicating that the Ag-Ag interaction dictates the overall structure. Based on atomically resolved STM images of the $c(10\times2)$ superstructure, a structural model is presented, and a mechanism is suggested which explains how the surface alloy phase is converted into the overlayer structure. [S0163-1829(96)05836-5]

I. INTRODUCTION

Heteroepitaxial metal-on-metal growth has been studied intensively for decades, mainly due to the unique catalytic, electronic, and magnetic properties of the resulting thin films. However, an essential corequisite to the understanding of these types of phenomena is a determination of the growth mechanism and the resulting surface and interfacial structure. In many early studies, the growth morphology of a given heteroepitaxial system was often predicted from thermodynamic equilibrium considerations, that is, from the respective surface free energies of the admetal (γ_A) and substrate (γ_B).[1,2] However, details regarding the specific atomic structure of the ensuing monolayer admetal have proven difficult to predict. Recent experimental and theoretical investigations have discovered a wide complexity of surface structures among differing heteroepitaxial monolayer systems. This complexity arises from such effects as, (i) the accommodation of large interfacial (γ_{AB}) and strain energies,[3,4] (ii) the formation of confined surface alloys in systems where there is bulk immiscibility,[5,6] and (iii) the reconstruction of the underlying substrate in the interfacial region.[7]

For the present Ag-Cu system, since $\gamma_{\text{Ag}} \ll \gamma_{\text{Cu}}$,[8] and there exists a large miscibility gap in the bulk phase diagram, one would expect from simple thermodynamic equilibrium arguments that silver would form a simple overlayer structure on the Cu(100) substrate. However, due to the large lattice mismatch (13%) between Ag (4.09 Å) and Cu (3.62 Å), the resulting overlayer is expected either to be highly strained, in the case of pseudomorphic growth, or to adopt a superstructure which is either commensurate or incommensurate to the underlying surface lattice.

As early as 1968, Palmberg and Rhodin[9] identified a $c(10\times2)$ low-energy electron-diffraction (LEED) pattern upon deposition of 1 ML of Ag onto the Cu(100) substrate. To explain this diffraction pattern, they proposed that the silver atoms formed a close-packed, hexagonal Ag(111)-like overlayer structure on the underlying Cu lattice; that is, the adlayer structure differs from the substrate two-dimensional square crystallographic symmetry. Subsequent investigations have corroborated this early assessment. In a series of angle-resolved photoemission experiments, Tobin *et al.*[10] investigated the development of the 2D band spectra of the strained Ag(111) overlayer in the monolayer region. Black *et al.*,[11] using electron-energy-loss spectroscopy, studied the surface lattice dynamics of the pseudo-Ag(111) overlayer, and compared the results with molecular-dynamics simulations using potentials from the embedded-atom method. More recently, experiments employing both impact collision ion scattering[12] and full-hemispherical photoelectron diffraction[13] have confirmed this earlier proposed model for the $c(10\times2)$-Ag-Cu(100) structure. Theoretically, Mottet, Tréglia, and Legrand,[14] using a tight-binding molecular-dynamics scheme, also concluded that the pseudohexagonal (10×2) structure was the lowest-energy configuration. Moreover, it should be pointed out that the Ag-Ni(100) (Refs. 15–17) and Au/Ni(100) (Ref. 18) systems have been shown to adopt a hexagonal overlayer structure [i.e., $c(8\times2)$] very similar to that of the Ag-Cu(100) system in the monolayer region. In each of the above indicated studies, the possibility of a surface alloy formation was excluded or negated, that is, within the monolayer region. It has previously been concluded that Ag does not intermix with the Cu(100) surface, but rather exclusively forms a simple overlayer structure.

In the present paper, we have utilized variable-temperature scanning tunneling microscopy (STM) to study the nucleation and growth of Ag on Cu(100), and the resulting structures, ranging from the submonolayer region to multilayer growth. In contrast to the previous studies referenced above, the present STM studies reveal that for subsaturation coverages Ag forms a layer-confined surface alloy even at temperatures as low as 300 K, which is below the dissolution temperature for Ag in Cu previously reported, namely, 450 K.[13,19] The results indicate that only ~0.13 ML

of Ag can be alloyed into the Cu surface. At higher Ag coverages, the large, silver-induced strain field is minimized by a condensation of Ag-$c(10\times2)$ patches within the Cu surface layer. When the Cu surface is saturated by the first Ag layer ($\theta_{Ag}=0.9$ ML), the Ag-Cu surface alloy mechanism is inoperative, and instead the Ag-$c(10\times2)$ superstructure is formed *on top* of the Cu substrate. A mechanism for the transition from the initial alloy to the formation of the $c(10\times2)$ superstructure is discussed. Moreover, based on atomically resolved images, a detailed structural model of the pseudohexagonal Ag $c(10\times2)$ structure will be presented and compared with previous reported structural models. Finally, the propensity for and identification of the formation of a Ag-Cu surface alloy will be discussed in light of results of both previous experimental studies and recent results from effective-medium calculations.

The structure of this paper is as follows: In order to explain fully the details of the surface alloy formation, we will first discuss the structure of the $c(10\times2)$ phase, both at saturation and subsaturation coverages at lowered temperatures (Sec. III A). Thereafter, the surface alloy phase and consequent transition to the $c(10\times2)$ phase will be discussed (Sec. III B), after which the experimental observations the growth morphology of the multilayer overlayers will be addressed (Sec. III C). Finally, the results will be discussed in relation to effective-medium theory calculations and compared with previously published literature (Sec. IV)

II. EXPERIMENTAL DETAILS

The results described here were performed in an UHV chamber (base pressure of 5×10^{-11} mbar) equipped with a fully automated, high stability ($\Delta z<0.01$ Å) scanning tunneling microscope,[20] as well as standard facilities for surface cleaning and characterization (LEED, single-pass cylindrical mirror analyzer, ion sputter gun). All STM images presented here were recorded in the constant-current mode using single-crystal tungsten tips. Typical tunneling currents were $\sim\pm1$ nA, with bias voltages in the ±1- to ±100-mV range. The STM has recently been modified such that STM imaging can be performed with the sample at temperatures ranging from 120 to 350 K. Heating is accomplished with 75-V zener diodes, while the cooling system is a liquid-nitrogen-cooled Al reservoir block connected via Cu braids to the STM sample holder. The latter is isolated from the rest of the STM with three quartz balls (1-mm diameter).

The Cu(100) crystal, having a miscut of $\leqslant0.5°$, was cleaned by repeated cycles of room-temperature (RT) 1–2-keV Ne^+ sputtering and subsequent annealing to 825 K. Sample cleanliness was monitored with both Auger electron spectroscopy (AES) and STM. At the end of the cleaning cycles, (1×1) LEED patterns were quite sharp, with low background. Using both AES and STM, individual surface contaminants (e.g., C, O, or S) were determined to be well below 1%. Silver was vaporized from a hot W conical wire onto the Cu substrate, which was held at a constant temperature. During deposition, chamber pressure remained below 2×10^{-10} mbar. The reported silver coverages are relative to the density of the underlying Cu(100) surface (1-ML Ag$=1.53\times10^{15}$ atoms/cm^2), rather than to the Ag(111) surface density (1.38×10^{15} atoms/cm^2). Upon determination of the local Ag structure, the reported macroscopic coverages were obtained by measuring the island density from large-scale STM images. The Ag deposition rate was typically adjusted to be between 0.002 and 0.005 ML/s. Post-annealing cycles entailed raising the sample at a rate of ≈2 K/s to the desired temperature for ≈300 s, and then recooling it to the desired temperature within the STM.

III. RESULTS AND INTERPRETATION

A. Details of the $c(10\times2)$ structure between 150 and 450 K

There is an inherent complication in studying Ag on Cu(100) with conventional STM, namely, the low barrier for Ag adatom diffusion on terraces and along steps. Although direct experimental diffusion data are not available, molecular-dynamics simulations,[21] using corrected effective-medium theory, indicate a very small diffusion barrier in the case of Ag on Cu(100). Specifically, of the nearly 50 permutations of adatom–substrate combinations, this study indicated only Ag on Ag(100) has a lower diffusion barrier. This explains why, at 300 K and for low Ag coverages ($\lesssim0.4$ ML), we find that atomically resolved STM imaging of the surface is nearly impossible. Typically, STM images show only noise, attributed to the high Ag adatom-cluster diffusion, on the Cu-(1×1) surface. Consequently, the atomic structure of the Ag-Cu(100) surface cannot be deduced at these conditions. There are two ways to overcome this problem: Either to perform the STM imaging at a lower temperature, whereby the adatom and/or island diffusion is reduced or to focus on surface conditions for which the Ag coverage is at or nearly at saturation. In this way the Ag overlayer is ''locked'' in, and the Ag mobility subsequently eliminated.

As mentioned above, we will begin by presenting STM results for the $c(10\times2)$ superstructure employing both of these two experimental approaches. Figure 1 shows STM images, acquired at 300 K, after the surface is saturated with a full overlayer of Ag at 300 K, and subsequent post-annealing to 425 K, reasons for which are elaborated in Sec. III C. As seen in Fig. 1(a), fairly large, flat domains of the silver overlayer structure are produced. The apparent height of the step edge, that runs vertically in the left-hand side of the image, is consistent with a Cu step height of 1.8 Å, indicating that the first layer of Ag homogeneously ''wets'' the underlying Cu(100) substrate. This is consistent with what one would expect thermodynamically due to the lower surface free energy of the Ag overlayer. At higher resolution [Figs. 1(b) and 1(c)], the atomic arrangement of the first Ag overlayer is seen to be highly ''buckled'' along one of the underlying Cu high-symmetry directions; in Fig. 1(b) the ''buckled'' direction of the adlayer is aligned along the Cu-[011] direction. Two orthogonal domains of the overlayer structure are observed consistent with the twofold symmetry of the Cu(100) lattice. Although single domains usually traverse the full Cu terraces, which typically have a width of several hundred Å, domain boundaries do sometimes occur on large terraces, as shown in Fig. 1(c). To avoid confusion between the two domains, we will adopt the domain symmetry indicated by the arrow in Fig. 1(b).

The details of the atomic structure are depicted in Figs. 1(b), 1(c), and 1(d). The striking characteristic of the atomically resolved images is the large modulation of any given

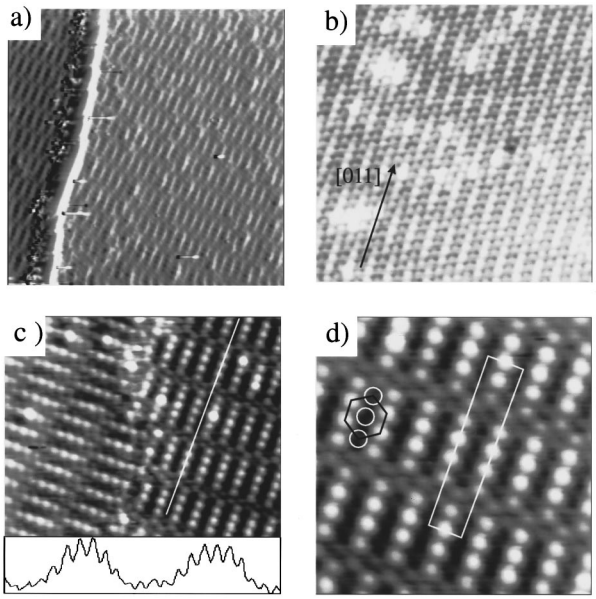

FIG. 1. STM images, acquired at 300 K, of the Cu(100) surface after depositing a monolayer of Ag and annealing to 425 K: (a) flat Ag-covered terrace with underlying Cu step edge (left side) [(160 $\times$160 Å^2)]; (b) atomically resolved ''buckling'' of the Ag overlayer along the Cu high-symmetry direction (80$\times$80 Å^2); (c) same, but showing domain boundary and height linescan (full-scale height, 0.75 Å), with a modulation period and amplitude of 25.6 and $\sim$0.40 Å^2, respectively (80$\times$80 Å); (d) atomically resolved details of the Ag-(10$\times$2) superstructure and local pseudohexagonal arrangement (40$\times$40 Å^2).

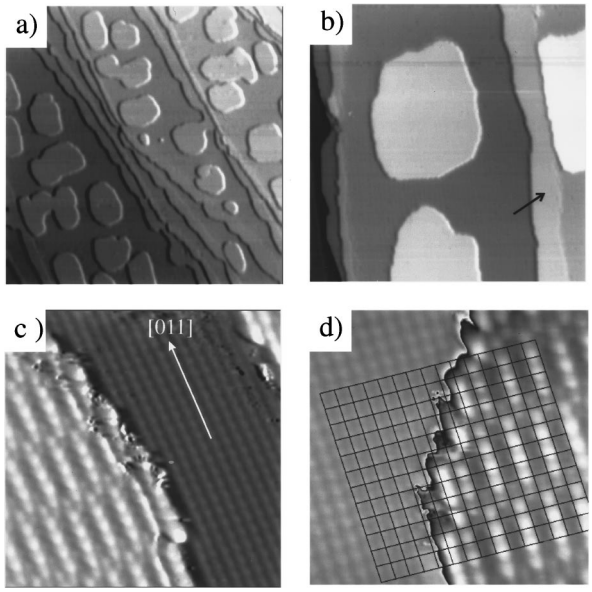

FIG. 2. STM images, acquired at 160 K, of the Cu(100) surface after depositing a subsaturation coverage (θ_{Ag}=0.4 ML) of Ag at 225 K: (a) large-scale image indicating the formation of Ag islands decorating Cu terraces and step edges (2300$\times$2300 Å^2]); (b) same, but note the Ag island's height compared to the Cu step edge [see arrow; the reader is referred to Fig. 8(a), which diagrammatically shows a horizontal linescan representing the area immediately below the arrow in the (STM image) (760$\times$760 Å^2); (c) atomically resolved image showing islands consisting of the Ag-c(10$\times$2) overlayer structure surrounded by clean Cu(100) terraces (54$\times$54 Å^2); (d) Cu-(1$\times$1) grid overlaid on the Ag island reveals the superstructure registry (38$\times$38 Å^2).

Ag row along the [011] direction, as shown in the line scan at the bottom of Fig. 1(c). The measured amplitude of the oscillation is $\sim$0.40 Å, and the wavelength is $\sim$26 Å. It is also observed that the sinusoidal modulation of adjacent Ag-[011] rows is 180° out of phase, so that, when one row is depressed, the adjacent rows are protruded. At the nodes of this modulation, the height of adjacent rows are nearly equivalent. The measured distance between any two Ag-[011] rows is 2.56 Å, consistent with a pseudomorphic epitaxial arrangement of the Ag layer with respect to the underlying Cu lattice, for which the nearest-neighbor Cu-Cu distance is 2.56 Å. The modulation wavelength along the [011] direction ($\sim$26 Å) is consistent with a commensurate 10-Cu[011] unit-cell distance (25.6 Å). Based on this, we can conclude that the superstructure has a c(10$\times$2) unit cell, consistent with early LEED diffraction results. For clarity reasons, a p(10$\times$2) unit cell is superimposed in Fig. 1(d). Although the gross features of the superstructure follow the twofold symmetry of the underlying lattice, it can be seen from Fig. 1(d) that each Ag atom lies in a near-hexagonal arrangement. In this image the depressed Ag atoms are not visible, whereas in Fig. 1(b), recorded under different tunneling conditions, they can be seen. The Ag-Ag distance along the Cu-[011] direction is measured, on the average, to be 2.85$\pm$0.02 Å, slightly contracted from the bulk nearest-neighbor Ag-Ag distance of 2.89 Å.

Before a definitive structural model can be constructed, the registry of the overlayer with respect to the underlying lattice must be determined. This can be accomplished by concurrently imaging both the Cu substrate and the Ag-c(10$\times$2) structure. Due to the large Ag adatom mobility at room temperature, this procedure can only be carried out at a lower temperature. Figures 2(a) and 2(b) show large-scale STM images, scanned at 160 K, of the Cu(100) surface after deposition of a submonolayer coverage of Ag at 225 K. On this highly stepped surface region, one sees that Ag islands ($\sim$250$\times$250 Å^2) are formed on the terraces, and that Ag decorates descending Cu step edges [indicated by an arrow in Fig. 2(b)]. Higher resolution images [Figs. 2(c) and 2(d)] show that these Ag islands consist of the same c(10$\times$2) structure as the one seen at the Ag saturation coverage at room temperature. Atomic-scale images of the region between the Ag islands [Figs. 2(c) and 2(d)] show a flat Cu(100) substrate. Thus at these lower temperatures, Ag adopts a simple overlayer structure even at subsaturation coverages and no indication of Ag intermixing with the Cu substrate is observed. Note that island shapes are, in general, compact, and that is there is no indication of fractile shape as has been identified in other heteroepitaxial systems,[3,22,23] indicating a fast vacancy-kink diffusion along the perimeter of the Ag islands. At this low temperature (160 K), the height of the Ag-c(10$\times$2) islands is measured to be 2.25 Å, a value which is close to the step height on the Ag(111) surface (2.36 Å), but significantly larger than the Cu(100) step height [see Fig. 2(b)]. To extract the registry of the Ag structure with respect to the Cu(100) lattice, a Cu-(1$\times$1) grid has been extended over the Ag-c(10$\times$2) island in Fig. 2(d). Such a grid reveals two important structural details. First, the Ag-

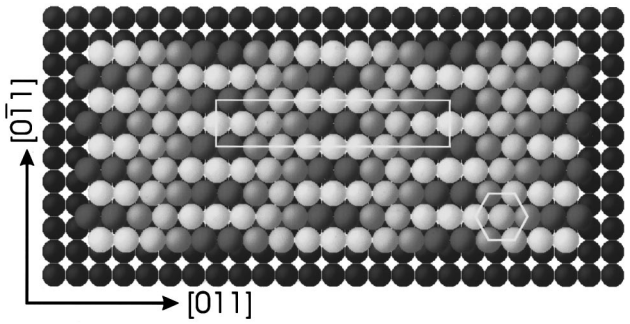

FIG. 3. Atomic model of the Ag-$c(10\times2)$ overlayer suggested by STM data. Color scale reflects the hard ball height above the flat Cu surface (assuming $r_{AG}=1.45$ Å and $r_{Cu}=1.28$ Å). Both Ag(10×2) and pseudo-Ag(111) unit cells are indicated.

[011] overlayer rows are geometrically constrained to adopt a pseudomorphic arrangement with respect to the underlying Cu atomic rows along the Cu-[011] direction. Second, the Ag atoms occupying near Cu bridge sites are observed to be imaged higher.

These two observations allow us to present a structural model for the Ag-$c(10\times2)$ overlayer on Cu(100) which explains the STM observations. Figure 3 shows a hardball model of the pseudohexagonal Ag structure. In this model the Cu(100) substrate is constrained to be flat. As indicated in the STM images, the Ag-[011] rows have been constrained to lie within the Cu-[011] troughs, while the Ag-Ag bond distance (2.84 Å) along these rows has been set to achieve the 10-Cu unit-cell periodicity. This packing sequence produces a local coverage of 0.9 ML for the Ag-$c(10\times2)$ superstructure; again a $p(10\times2)$ unit cell is indicated in Fig. 3. The color scale used in the model refers to the height one would expect if a near Ag(111) overlayer were placed over a Cu(100) substrate (as in the STM images, darker is depressed, lighter is protruded). The hardball height corrugation (~0.36-Å maximum) between Ag atoms occupying near-bridge and hollow sites agrees relatively well with that measured by STM (~0.40 Å). The theoretical investigation by Mottet, Tréglia, and Legrand[14] predicted a much smaller corrugation amplitude, namely, 0.2 Å, primarily due to a rather large outward relaxation of the Ag overlayer ($\Delta d_0=+11\%$); this assessment does not seem to be corroborated by our STM data. Note that the overall observed characteristics of the model are consistent with the STM images. One can identify the out-of-phase buckling along the [011] direction, as well as the relatively flat nodal regions. Further details concerning the model will be discussed in Sec. IV.

B. Initial alloy formation and consequent formation of the Ag-$c(10\times2)$ phase >300 K

So far we have shown that a Ag-$c(10\times2)$ superstructure occurs at saturation coverage at or above 300 K, and a subsaturation coverages below 225 K. However, this structure does not nucleate and grow for all coverages and temperatures. As will be discussed below, at subsaturation coverages at or above 300 K, a surface alloy is formed from which the impinging Ag atoms squeeze out Cu atoms from the surface and subsequently alloyed in. This shows that the formation of the Ag-Cu surface alloy is an activated process.

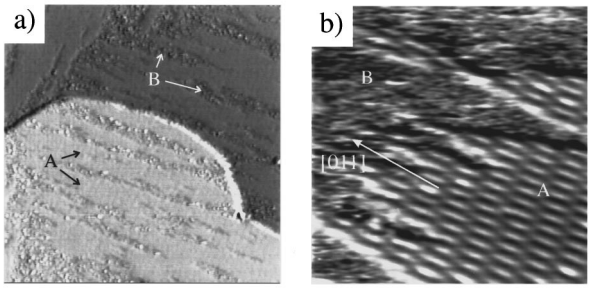

FIG. 4. STM images, acquired at 300 K, of the Cu(100) surface after depositing a subsaturation coverage ($\theta_{Ag}\approx0.75$ ML) of Ag at 475 K: (a) large-scale image, with the Cu step edge running horizontally, showing that the surface is composed of ''streaky patches'' (labeled *A*) separated by diffuse regions (labeled *B*) (550 ×550 Å^2); (b) smaller scale image reveals a previously identified Ag-$c(10\times2)$ superstructure in the patch region.

Figure 4 shows STM images, recorded at 300 K, of the Cu(100) surface after Ag is deposited to near-saturation coverage (~0.75 ML) at 475 K. What is readily apparent from Fig. 4(a) are large, elongated streaky patches on the surface (labeled *A*). As seen from Fig. 4(b), these patches correspond to the *A* regions of the $c(10\times2)$ structure with the characteristic buckling of adjacent rows. However, the patches have a height of only ~0.3 Å above the in-between flat areas (labeled *B*), which is significantly smaller than the height of the low temperature (225 K) deposited Ag islands shown in Fig. 2. The small height of the patches indicates that the $c(10\times2)$ structure is located *within* the Cu surface layer, in stark contrast to the lower-temperature data (<225 K) discussed above, in which case the $c(10\times2)$ structure is lying on top of the Cu surface.

Time-sequential STM images at 300 K reveal that the surface is highly dynamic. The phase boundaries between the Ag-$c(10\times2)$ patches and the flat regions separating them appears to be highly mobile caused by a concomitant 2D evaporation and from the subsequent condensation of the Ag to the $c(10\times2)$ patch. Because of this large motion, atomically resolved imaging of the regions between the patches is impossible at 300 K. However, this becomes feasible at lower temperatures.

Figure 5 shows a series of STM images, for which Ag was deposited at low temperature (225 K), annealed to 425 K, and subsequently recooled to 170 K. The Ag coverage, determined from the $c(10\times2)$ island density prior to the annealing sequence, is 0.4 ML. At this lower coverage, the Ag-$c(10\times2)$ regions are only ~20 Å wide. The elongated direction of the Ag patches corresponds to the buckling direction of the $c(10\times2)$ structure. From Fig. 5(a), it is found that the Ag-$c(10\times2)$ patches have a height of only ~0.3 Å above the surface, and that there are approximately equal areas of the patches following the two different domain possibilities. Although the total Ag coverage, as measured at low temperatures, is known to be 0.4 ML, the Ag-$c(10\times2)$ patches in Fig. 5(a) obtained after the annealing sequence only comprise an area equal to a Ag coverage of ~0.27 ML. It is proposed that this Ag deficit (~0.13 ML) is alloyed into the interpatch region. In Figs. 5(b) and 5(c), atomically resolved imaging of the small $c(10\times2)$ regions, indicated by arrows, are observed. In Fig. 5(c), an enlarged image of a Ag

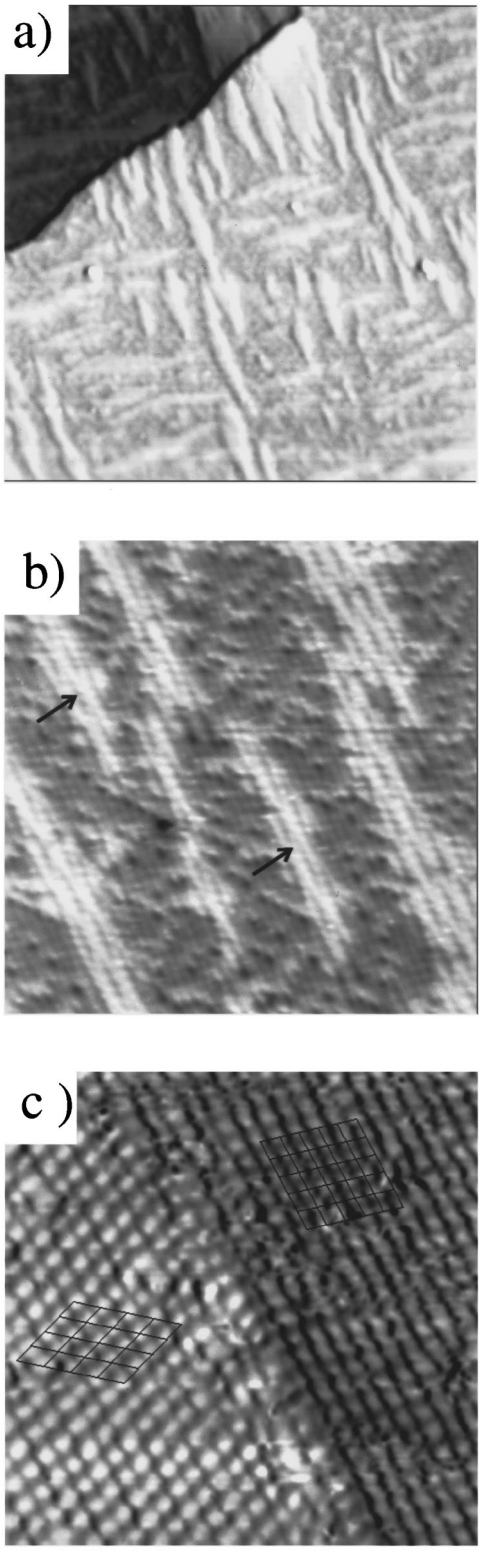

FIG. 5. STM images, acquired at 170 K, of the surface after depositing 0.4 ML of Ag at 425 K and subsequently annealing: (a) large-scale image, with monoatomic step edge in upper-left corner, showing anisotropically shaped ''patches'' directed along both Cu high-symmetry directions (540×540 Å^2); (b) atomically resolved image showing local Ag-(10×2) structure within patch region (indicated by arrows) (120×120 Å); (c) smaller scale image revealing hexagonal Ag-c(10×2) superstructure at left [with Ag(111) grid], and Ag-Cu alloy at right [with Cu-(1×1) unit grid] (58×58 Å^2).

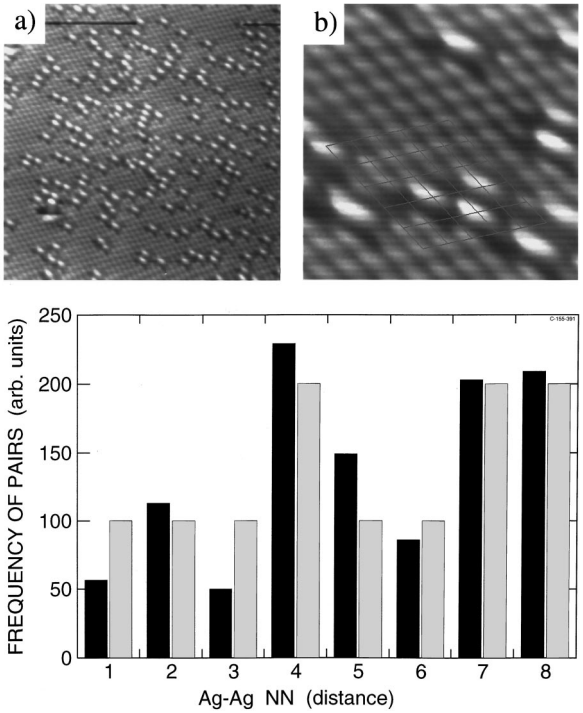

FIG. 6. STM images, acquired at 180 K, of the Cu(100) surface after depositing a very low coverage (θ_{Ag}=0.07 ML) of Ag at 440 K: (a) large-scale image showing Ag, seen as protrusions, alloyed in the Cu surface (125×125 Å^2); (b) Cu-(1×1) unit grid showing alloyed Ag is pseudomorphically constrained within the Cu(100) surface (60×60 Å^2); (c) pair-correlation plot of the nearest-neighbor (NN) distribution of Ag atoms from (a) (Ref. 35).

patch (left) and an in between region (right) is shown. Because of differing tunneling conditions, the Ag-c(10×2) region in this image appears flat instead of buckled as above, revealing only the Ag hexagonal arrangement of atoms (see superimposed grid). As shown by the superimposed grid on the right-hand side of Fig. 5(c), the region adjacent to the c(10×2) patch appears to have Cu-(1×1) symmetry. This indicates that 0.13 ML of Ag is substituted into the topmost Cu(100) surface in the regions in between the patches of Ag. The depressions in the Cu-(1×1) region next to the Ag-c(10×2) patches, corresponds to an approximate local coverage of 0.13 ML, and thus are associated with the Ag atoms alloyed into the topmost Cu(100) surface layer.

To further confirm that Ag indeed intermixes with the Cu(100) surface, and forms a surface alloy at low coverage (<0.13 ML), a series of experiments were performed at much lower Ag coverage. Figure 6 shows the Cu(100) surface with only 0.07 ML of Ag deposited at 440 K and subsequently scanned at 180 K. The Ag appears from the image to show up as protrusions in the surface and, from the superimposed Cu(1×1) grid in Fig. 6(b), it can be concluded that the Ag atoms occupy substitutional Cu sites. This demonstrates that the Ag forms a direct substitutional surface alloy at this low coverage. The reason why Ag atoms show up as protrusions in Fig. 6 and as depressions in Fig. 5 is a consequence of a different tip configuration, e.g., a clean W tip as opposed to an electronegative atoms bound at the tip apex. Similar changes in contrast between the heteroepitaxial species are found in the literature.[5,24,25] The height of the Ag

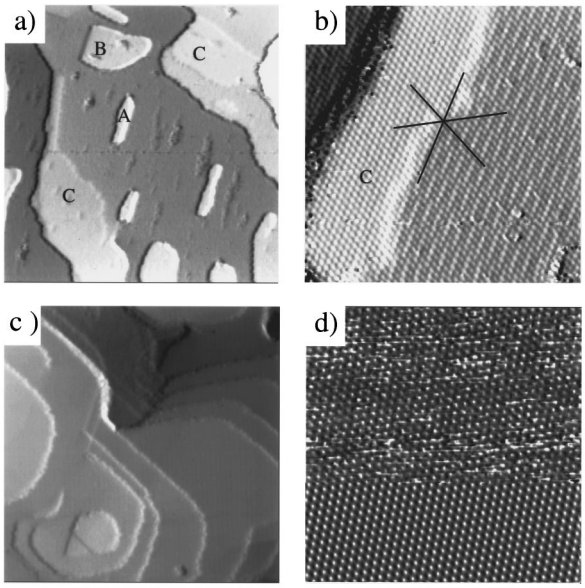

FIG. 7. STM images, acquired at 300 K, of the Cu(100) surface at Ag coverages above the first monolayer: (a) large-scale image showing rough morphology after depositing of 1.2 ML of Ag at 300 K (550×550 Å^2); (b) same, but showing the atomic structure of a second layer of Ag (labeled *C*) (120×120 Å^2); (c) large-scale image showing 3D island growth morphology after deposition of approximately 5 ML at 300 K (800×800 Å^2); (d) same, but showing atomically resolved image after annealing to 550 K (bottom one-third of image corresponds to a unit cell averaging of upper two-thirds) (80×80 Å^2).

protrusions above the Cu lattice in Fig. 6 is ~0.25 Å, and agrees well with the height difference found for other similar surface alloy systems studied with STM [Au-Cu(100), ~0.2 Å;[24] Pd-Cu(100), ~0.2 Å;[25] $Pt_{25}Ni_{75}$(100), ~0.3 Å (Ref. 26)].

From STM images similar to that shown in Fig. 6(a), a pair-correlation plot of the nearest-neighbor (NN) distribution of Ag atoms ranging out to a distance of eight NN positions can be constructed. The experimentally determined occupation probability of the alloyed Ag atoms, separated by NN Cu distances, are shown in Fig. 6(c), and, for comparison, the same type of distribution is shown corresponding to a purely random distribution of the Ag atoms within the Cu substrate. As seen from the plot, there is a pronounced attenuation of the number of Ag atoms occupying certain NN distances. Specifically, the number of Ag atoms separated by one and three NN distances is only one-half of what one would expect from a purely random array. This indicates a strong short-range repulsive interaction between Ag atoms located along the [011] and [011] directions, respectively. Note that, from the plot, there is no increased second-NN Ag-Ag pairing which would indicate a propensity for a $c(2\times2)$ formation which has been identified for both the Pd-Cu(100) (Ref. 25) and Au-Cu(100) (Ref. 24) systems.

C. Growth morphology for Ag coverages above 0.9 ML and at temperatures at or above 300 K

Figure 7(a) shows a large-scale image, recorded at 300 K, of the Cu(100) surface upon deposition of approximately 1.2 ML Ag at 300 K. As opposed to the case where a post-annealing sequence produced large, flat terraces of the Ag-$c(10\times2)$ structure (see Fig. 1), this unannealed surface has a fairly rough surface morphology. Small and large islands are observed on the terraces [labeled *A* and *B* in Fig. 7(a)], the step edges are rough and not aligned with the low-index directions of the underlying lattice, and, most importantly, there is an indication of another structure near step edges (labeled *C*). Atomic scale imaging indicates that the surface is predominantly dominated by the $c(10\times2)$ superstructure, which exists both at the terraces and on the islands. The small regions containing structure *C* have an apparent height of 0.4 Å above that of the adjoining terraces, and, as shown in Fig. 7(b), this structure has the same lateral hexagonal symmetry as the $c(10\times2)$ structure [see the intersecting lines in Fig. 7(b)], but there is no indication of the large buckling corrugation. These structural *C* regions appear to have a structure nearly identical to a flat Ag(111) surface.

The structural region *C* is believed to be associated with a second layer of Ag islands, showing an apparent lack of the buckling seen in the first Ag layer structure. A hardball model, similar to that presented in Fig. 3, suggests that, if the first Ag layer retains the magnitude of the buckling, the subsequent second Ag layer should also possess a similar buckled superstructure although smaller in magnitude. This effect is not observed. Although STM data cannot conclusively yield structural information of the interfacial region in this case, and hence one must consider the proposal tenuously, it appears that the deposition of the second Ag layer may indeed lead to a flattening of the underlying Ag layer. However, it should be added that because of the uncertainty in precisely determining the height of the islands, this cannot be fully confirmed, and hence calls upon other experimental studies which directly probe the interfacial structure.

Another important observation from Fig. 7(a) is that the surface structure of the small islands (*A* and *B*) also shows a characteristic buckled-$c(10\times2)$ Ag structure. Since the measured height of these islands above the surrounding $c(10\times2)$ Ag terrace is equal to a monoatomic Cu(100) step, the islands lie on top of a Cu island within the first Ag overlayer. This proposition is consistent with the mechanism suggested above, indicating that at 300 K the $c(10\times2)$ structure initially nucleates as a surface alloy and subsequently grows within the Cu surface layer. The small observed Ag islands [seen in Fig. 7(a)] appear to lie on top of the kinetically pinned Cu(100) island within first Ag layer. As discussed previously, the terraces become flat upon annealing to 425 K; that is, the trapped Cu atoms under the islands flow to step edges, and thereupon are covered by the Ag-$c(10\times2)$ overlayer.

At higher coverages and at deposition temperatures of 300 K, STM reveals a multilayer 3D island growth morphology. As shown in the large-scale image [Fig. 7(c)], many partial layers of large clusters are observed. This image, acquired at 300 K, corresponds to an average Ag coverage of ~4.5 ML. It is important to note that the ascending islands have step edges which are characteristic of threefold symmetry, as opposed to the twofold symmetry of the substrate. This is consistent with the subsequent growth of Ag on Ag(111) islands. Upon annealing to 575 K the surface morphology becomes somewhat more flat, although it corresponds to a 3D multilayer as opposed to a 2D layer-by-layer growth mode.

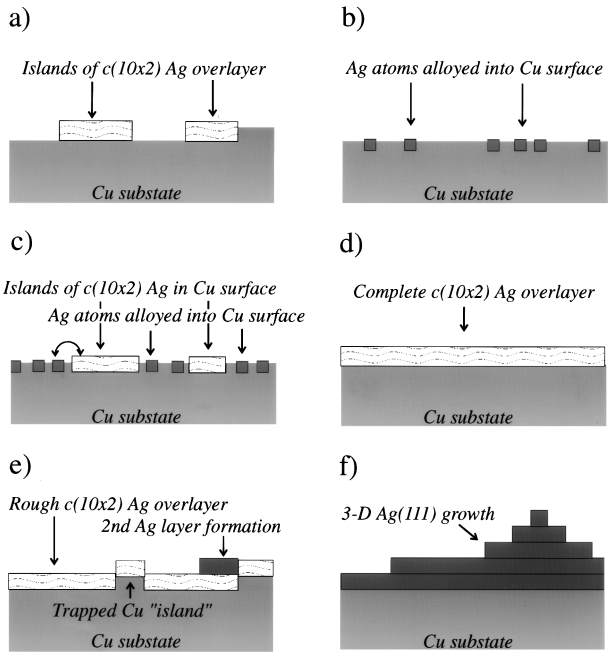

FIG. 8. Models describing Ag growth on Cu(100) as a function of temperature and coverage: (a) low-temperature (<200 K) Ag-$c(10\times2)$ overlayer at monolayer coverages; (b) Ag-Cu surface alloy above 300 K at low coverages; (c) coexistence of Ag-Cu alloy and Ag-$c(10\times2)$ phases within a Cu surface at medium coverages (>300 K); (d) flat Ag-$c(10\times2)$ overlayer at saturation of first layer upon annealing; (e) at room temperature, ''rough'' surface morphology ($0.85<\theta_{Ag}<2$ ML); (f) 3D Ag(111) islands at higher coverages (>3 ML).

Figure 7(d) shows an atomically resolved STM image of the annealed surface, with a unit-cell average of the structure at the bottom. The surface is seen to have a hexagonal Ag overlayer symmetry, with a measured Ag-Ag bond distance equal to that of the bulk Ag(111) (2.89 Å).

IV. DISCUSSION AND SUMMARY

Based on our STM findings, we now summarize the overall nucleation growth of Ag on Cu(100) as a function of both Ag coverage and temperature. At low temperatures (<225 K), deposition of Ag leads to the formation of the $c(10\times2)$ superstructure which lies *on top* of the Cu substrate. As shown in Fig. 8(a), there is no indication of any alloy formation, and because of the lower mobility at these temperatures, Ag forms compact islands both separated from and adjoined to Cu step edges. Thus, below 225 K, Ag forms a close-packed, hexagonal *overlayer* structure.

The situation is much different for temperatures at or above 300 K. Here we find that the structural arrangement in the low-coverage region (<0.13 ML) is the formation of a surface alloy [Fig. 8(b)]. The alloyed Ag atoms are substitutionally arranged *within* the Cu(100) surface lattice. The fact that this surface alloy forms only at temperatures above 300 K and not at lower temperatures shows that the formation of the surface alloy phase is an activated process. At medium coverages ($0.13\leqslant\theta_{Ag}<0.7$ ML), it appears that a fraction of the Ag segregates into the $c(10\times2)$Ag patches lying *within* the Cu surface layer, and indicates a ''dealloying'' mechanism. This is diagrammatically shown in Fig. 8(c). However, in the region between the $c(10\times2)$ regions, the Ag atoms remain in the substitutional surface alloy phase at a local surface concentration of ~0.13 ML; that is, there is a phase segregation between the Ag-$c(10\times2)$ superstructure and the surface alloy phase. This observation suggests that there is a local coverage limit to how much Ag can be intermixed into the Cu surface.

At saturation coverage (0.9 ML), the entire flat surface adopts the $c(10\times2)$ structure if the deposition temperature is above 425 K [see Fig. 8(d)]. Again there is no indication of surface alloy formation; rather, it appears that the Ag atoms form a simple overlayer configuration. At lower deposition temperatures (300 K), a rougher growth morphology is observed [see Fig. 7(a)], because a portion of the alloy-ejected Cu atoms coalesce on terraces rather than accommodate at interfacial Cu step edges. Due to this effect, Cu islands are kinetically constrained within the first Ag layer and thus act as a template for smaller Ag-$c(10\times2)$ islands on top, as shown in Fig. 8(e). Furthermore, the formation of a second Ag layer is observed under these conditions, and they appear to be relatively flat compared to the highly buckled $c(10\times2)$ first-layer Ag structure, but both structures have a local hexagonal substructure. Subsequent higher coverages lead to the formation of what can be described as multilayer 3D Ag-Ag(111) growth [Fig. 8(f)].

This study reveals that Ag forms a limited (≈0.13 ML) surface alloy with Cu(100) at temperatures above 300 K. This result conflicts with that proposed in earlier studies,[12,13] where it was concluded that no alloy formation occurs. However, these earlier results were based on the observation that no alloy structure was observed at the completion of the first Ag layer. The present STM results confirm this latter assessment, but also show that at low Ag coverages the mechanism for the $c(10\times2)$ structural formation is driven by an initial alloy formation of Ag in the first Cu(100) layer.

Recent effective-medium-based calculations of various heteroepitaxial systems[27] confirm that within the low-coverage limit the lowest-energy configuration is a Ag-Cu surface alloy. Specifically, the authors predict that the energy for a Ag adatom on the Cu(100) lattice is 0.10 eV/atom, whereas if the atom is alloyed into the first Cu layer, the energy is much lower (−0.36 eV/atom) if one accounts for the reaccommodation of the displaced Cu atom into a large Cu island; the energy stated is measured relative to the cohesive energy of the guest atom. This calculation predicts that the energy of a Ag hexagonal overlayer is −0.17 eV/atom. Although this value is higher, the energy of the surface alloy corresponds to isolated Ag atoms within the Cu surface. Our STM results show that the maximum concentration of isolated alloyed Ag is limited (<0.13 ML), and hence indicate that as more alloyed Ag is accommodated in the surface layer, the increasing compressive stress induced by the Ag drives the alloy energy upwards. At a critical coverage, the hexagonal buckled Ag-$c(10\times2)$ phase then becomes the lower-energy structure.

It should be noted that this theoretical study also predicted that the energy of a Ag atom alloyed into the second Cu layer is much higher (−0.06 eV/atom), and comparable to the calculated bulk alloy (−0.04 eV/atom). Thus from both our STM data and these calculations, it appears that the alloy

is confined within the surface region only. The phenomena of surface-confined alloy formation has been identified in many other heteroepitaxial systems including Ag-Pt(111) (Ref. 4) and Fe-Cu(100),[28] both bulk miscible, and Au-Ni(110),[6] which is bulk immiscible. In each of these systems, a clustering of alloyed admetal atoms was observed within the first substrate layer. In the present case, when the Ag concentration within the first layer becomes greater than 0.13 ML, a similar clustering results. However, in this case the clusters exhibit a different structural arrangement, i.e., the $c(10\times2)$ phase. In a theoretical study by Tersoff,[29] this type of phenomenon arises from a positive interfacial energy term ($\gamma_{AB}>0$) which drives a lateral segregation of a guest atom A into the surface layer. For the Ag-Cu(100) system, we see the opposite effect. That is, in the low-coverage region, individual alloyed Ag atoms repel each other due to the ensuing strain fields in the near vicinity. From the observation of a limited alloy formation ($\sim$0.1 ML), there appears to be a limit to which this strain field can be accommodated in a Cu surface lattice. The field is minimized by the formation of the pseudohexagonal structure within the first layer. This mechanism can be viewed as a ''alloy$\rightarrow$dealloy'' process, wherein the dealloyed phase corresponds to the $c(10\times2)$ phase located *within* the Cu surface layer. A very similar mechanism, based on STM data, has been proposed for both the Au-Ni(110) (Ref. 5) and Pb-Cu(111) (Ref. 30) systems.

The proposal that ''compressive stress'' dictates the Ag alloy to $c(10\times2)$-superstructure phase transition at a critical coverage (0.13 ML) is corroborated by a similar explanation for the initial surface alloy formation. From simple charge-redistribution arguments, by and large, the tension of a clean metallic surface is positive (tensile). In agreement, Rayleigh phonon-dispersion measurements of clean Cu(100) indicate a surface tensile stress.[31] Interestingly, in response to this stress, a recent LEED-IV structural analysis of the Cu(100) surface identified a lateral 1% contraction (tensile strain).[32] Using a simple ''size-effect'' argument, Schmidt *et al.*[33] indicated that in systems under surface tensile stress, the energy is minimized by an effective atomic size in the surface layer larger than that of the corresponding bulk. This study reported that in the theoretical case of Pd(111) and Pd(100), the energy is minimized with first-layer atoms being 1.4% and 2.9%, respectively, ''larger'' than bulk atoms; moreover, if the effective size is larger than this, the surface reverses to a compressive stress. Similarly, in the present Ag-Cu system, the tensile stress of the clean Cu surface is originally relieved by the incorporation of the larger-size Ag atom. At the critical coverage of 0.13 ML, the average size of the Ag-Cu surface atoms is 1.7% larger than bulk Cu, a value that compares well with the theoretical values for the Pd surfaces.[31] Above this critical coverage, further incorporation of Ag increases the average surface atom size, and hence the surface becomes compressive.

We now discuss the details of the overlayer structure. At saturation coverage, the silver adopts a structure nearly equivalent to a Ag(111) surface. Specifically, along the [011] direction, it is seen that nine Ag atoms reside over a ten-Cu-atom spacing, which corresponds to a 1.6% contraction with respect to the bulk Ag-Ag distance. However, in the perpendicular direction, there is a dilation of the distance between adjacent Ag rows of 2.2% as compared the bulk Ag-[211] direction. Although this causes an anisotropic strain, the overlayer pseudohexagonal arrangement produces a lateral density within 0.6% of the Ag(111) surface. This propensity to form a $\sim$Ag(111) overlayer, independent of the substrate surface geometry, has been identified in many other similar systems. In the case of Ag-Cu(111) and Ag-Cu(110) systems[34] at saturation coverage, a highly buckled superstructure is observed, in which the Ag atoms are in a near Ag(111) arrangement.

In a simple model, the overlayer structure is dictated by two competing effects: substrate-adlayer and adlayer-adlayer interactions. If bonding between the substrate and adlayer strongly dominates, then, independent of the bulk lattice mismatch, the overlayer structure is locked pseudomorphically with the underlying lattice. If the adlayer-adlayer lateral interaction is greater than the substrate-adlayer interaction, an overlayer structure typically forms in which the nearest-neighbor adlayer distances are equal to their bulk counterparts. The Ag-Cu(100) system is more characteristic of this latter category, which indicates that the Ag-Ag interaction dictates the overlayer structure, or conversely, that the Cu-Ag interaction is weaker.

However, the situation is slightly more complicated than this simple assessment. The fact that the Ag atoms initially form a surface alloy phase, but subsequently dealloy at saturation coverage, forming a Ag(111) overlayer, indicates that the two phases are quite different. In the former case the strong, local Ag-Cu interaction leads to the formation of a surface alloy, whereas at saturation coverage, the Ag-Ag interaction dominates, leading to a overlayer structure which is nearly incommensurate with the underlying substrate. This is corroborated by other studies. Based on angle-resolved ultraviolet photoemission spectra data, Tobin *et al.*[10] found that the overlayer-substrate bonding of Ag-Cu(100) is dominated by the interaction with the delocalized Ag $5s$ states; furthermore, the Ag $4d$ bands showed only 2D dispersion, with little interaction with the substrate. Along with the structural data, this indicates that the Ag monolayer is almost free floating on top of the Cu substrate, wherein the long-range 2D Ag-Ag interaction dominates the overall atomic and electronic structure.

In summary, we have investigated with variable temperature STM the nucleation, growth, and structure of Ag on Cu(100) up to a multilayer coverage region. At temperatures below 250 K, Ag forms a pseudohexagonal, $c(10\times2)$ overlayer structure. However, at temperatures at or above 300 K, silver forms a substitutional surface alloy but only a limited amount of Ag, up to a coverage of 0.13 ML, can be alloyed into the Cu(100) surface layer. The fact that alloying only occurs at 300 K indicates that the formation of a surface alloy is an activated process. At higher coverages, because of the high induced strain energy, the alloyed Ag atoms phase separate into small patches of Ag-$c(10\times2)$ superstructure, that is, dealloy from the Ag-Cu surface. The alloy concentration limitation is determined by the increased strain energy which can be accommodated by the Cu surface lattice. At saturation coverage, the Ag-Ag interaction dominates the overall overlayer structure, forming a buckled $\sim$Ag(111) adlayer.

ACKNOWLEDGMENTS

We would like to acknowledge financial support from the Center for Atomic-Scale Materials Physics, sponsored by the Danish National Research Foundation, from the Danish Research Council through the center for Nan-tribology, and from the Knud Højgaard Foundation.

*Permanent address: Center for Advanced Microstructures and Devices (CAMD), Louisiana State University, Baton Rouge, LA 70803; email: sprunger@camd.lsu.edu

[1] E. Bauer and H. Poppa, Thin Solid Films **12**, 167 (1972).
[2] J. A. Venerables, G. D. T. Spiller, and M. Handbücken, Rep. Prog. Phys. **47**, 399 (1984).
[3] H. Röder, E. Hahn, H. Brune, J. Bucher, and K. Kern, Nature **366**, 141 (1993).
[4] H. Röder, R. Schuster, H. Brune, and K. Kern, Phys. Rev. Lett. **71**, 2086 (1993).
[5] L. P. Nielsen *et al.*, Phys. Rev. Lett. **71**, 754 (1993).
[6] L. P. Nielsen *et al.*, Phys. Rev. Lett. **74**, 1159 (1995).
[7] J. Jacobsen *et al.*, Phys. Rev. Lett. **75**, 489 (1995).
[8] F. R. deBoer, R. Boom, W. C. Mattens, A. R. Miedema, and A. K. Niessen, *Cohesion in Metals* (North-Holland, Amsterdam, 1988).
[9] P. W. Palmberg and T. N. Rhodin, J. Chem. Phys. **49**, 134 (1968).
[10] J. G. Tobin, S. W. Robey, L. E. Klebanoff, and D. A. Shirley, Phys. Rev. B **33**, 2270 (1986); **35**, 9056 (1987).
[11] J. E. Black *et al.*, Surf Sci. **217**, 529 (1989); J. E. Black and D. L. Mills, Phys. Rev. B **42**, 5610 (1990).
[12] S. Nakanishi, K. Kawamoto, and K. Umezama, Surf. Sci. **287/288**, 974 (1993).
[13] D. Naumoviv *et al.*, Surf. Sci. **307-309**, 483 (1994).
[14] C. Mottet, G. Tréglia, and B. Legrand, Phys. Rev. B **46**, 16 018 (1992).
[15] W. F. Egelhoff, J. Vac. Sci. Technol. A **6**, 730 (1988).
[16] A. Brodde *et al.*, J. Vac. Sci. Technol. B **9**, 920 (1991).
[17] J. E. Black, Z. Tian, and T. Rahman, Surf. Sci. **291**, 215 (1993).
[18] P. Statiris and T. Gustafsson, in *Structure of Surfaces IV*, edited by X. D. Xi, S. Y. Tong, and M. A. Van Hove (World Scientific, Singapore, 1994), p. 625.
[19] J. Eugéne, B. Aufray, and F. Cabané, Surf. Sci. **241**, 1 (1991).
[20] E. Lægsgaard, F. Besenbacher, K. Mortensen, and I. Stensgaard, J. Microsc. **152**, 633 (1988). The STM is a prototype of the Rasterscope 3000 from DME A/S, Denmark.
[21] D. E. Sanders and A. E. DePristo, Surf. Sci. **260**, 116 (1992).
[22] M. Bott, Th. Michely, and G. Comsa, Surf. Sci. **272**, 161 (1992).
[23] R. Q. Hwang, J. Schröder, C. Günther, and R. J. Behm, Phys. Rev. Lett. **67**, 3279 (1991).
[24] D. D. Chambliss and S. Chiang, Surf. Sci. Lett. **264**, L187 (1992).
[25] P. W. Murray, I. Stensgaard, E. Lægsgaard, and F. Besenbacher, Phys. Rev. B **52**, 52 (1995).
[26] M. Schmid, H. Stadler, and P. Varga, Phys. Rev. Lett. **70**, 1441 (1993).
[27] K. W. Jacobsen, P. Stoltze, and J. K. Nørskov (private communication).
[28] D. D. Chambliss, R. J. Wilson, and S. Chiang, J. Vac. Sci. Technol. A **10**, 1993 (1992).
[29] J. Tersoff, Phys. Rev. Lett. **74**, 434 (1995).
[30] C. Nagl, O. Haller, E. Platzgummer, M. Schid, and P. Varga, Surf. Sci. **321**, 237 (1994).
[31] M. Wuttig, R. Franchy, and H. Ibach, Z. Phys. B **65**, 71 (1986).
[32] S. Müller *et al.*, Phys. Rev. Lett. **75**, 2859 (1995).
[33] M. Schmid *et al.*, Phys. Rev. B **51**, 10 937 (1995).
[34] P. T. Sprunger and F. Besenbacher (unpublished).
[35] There is a small thermal drift in these images which distorts the observed square lattice.